SCVJ
Volume 4, Issue 2, 2023
DOI: https://doi.org/10.55989/TKOW2858
Science View Journal
ISSN (Online): 2734-2638

Maximum Power Point Tracking Improvement Using Model Reference Adaptive Control Scheme

I. I. Abraham, C. C. Mbaocha, S. O. Okozi

Department of Electrical and Electronic Engineering, Federal University of Technology, Owerri, Imo State, Nigeria

Email: isaac.abraham@futo.edu.ng

Abstract:
This paper presents maximum power point tracking improvement using model reference adaptive control (MRAC) scheme. Solar photovoltaic (PV) energy system remains one of the renewable energy applications which operate by tracking energy from the sun and converting it into useful electrical energy. However, harnessing the generated energy has been the major concern of the engineers hence the adoption of various control strategies for efficient control of the generated power. The idea is to transfer the optimal generated power to the output considering the fact that PV energy produced may have been affected by irradiation and temperature conditions. To avoid the unstable output power, there is need to deploy an efficient control scheme. Most of the conventional control techniques are not optimal to resolve power inaccuracies in the system and they have shortcomings. This work is therefore aimed at analyzing solar photovoltaic energy system using MRAC technique to investigate the control performance. The results obtained by simulation on MATLAB/Simulink software, show an average tracking efficiency of 73.41%, the rise time of 0.7093s and a duty cycle of 0.7. Moreover, MRAC operates at small gain values and the range at which MRAC can operate was found to be $0.1 < \Gamma < 2$.

Keywords: Adaptive control, improvement, maximum power point, model reference, solar photovoltaic energy, tracking.

I. INTRODUCTION

The photovoltaic (PV) power system is becoming increasingly important as the most available renewable source of energy since it is clean with little maintenance, low cost and without any noise, which is as a result of the absence of moving parts. Nevertheless, one of the issues associated with PV systems is the nonlinear characteristic of the power curve which change the amount of electric power generated. Unlike the traditional energy, solar energy is clean, inexhaustible and free. (Dolara,Faranda, & Leva, 2009). Photovoltaic (PV) systems are a critical component in addressing the national mandates of achieving energy independence and reducing the potentially harmful environmental effects caused by increased carbon emissions. (Khanna et. al., 2014).

Sometimes conventional feedback controllers may not perform well online because of the variation in process dynamics due to nonlinear actuators, changes in environmental conditions and variation in the character of the disturbances. To overcome such a problem, the design of a controller for a second order system with Model Reference Adaptive Control (MRAC) scheme using the MIT rule for adaptive mechanism was proposed. In this rule, a cost function is defined as a function of error between the outputs of the plant and the reference model, and controller parameters are adjusted in such a way so that this cost function is minimized. The designed controller gives satisfactory results, but is very sensitive to the changes in the amplitude of reference signal. It follows from the simulation work carried out in this paper that adaptive system becomes unstable if the value of adaptation gain or the amplitude of reference signal is sufficiently large. It has been observed that the response of the system improves with the increment in adaptation gain but beyond a certain limit ($0.5 < \gamma < 5$) the performance of the system becomes very poor. The selection of adaptation gain is very important and depends on the signal levels. (Jain & Nigam, 2013).

The development of model reference adaptive control for maximum power point tracking in PV systems by adopting a two-level control algorithm which are: ripple correlation control (RCC) and model reference adaptive control (MRAC) using Lyapunov approach showed an improved performance achieved with shorter time constants and overall system stability. (Vyshnavi & Subramanian, 2015). The researchers in their work developed a maximum power point tracking system using model reference adaptive control. In the work, a two-level control consisting of ripple correlation control (RCC) and the model reference adaptive control (MRAC) was carried out. The implication of the results obtained was that the proposed control algorithm enables the system to converge to the maximum power point in milliseconds. However, a large magnitude of control gain may lead to oscillations at the operating point. (Khanna et. al., 2014).

It has been discovered that fuzzy logic approach for maximum power point tracking gives an improved tracking with respect to the conventional P&O method but its disadvantage is that it is slow in power correction and fuzzy rules are predefined based on PV specifications. The real time experiment was done based on voltage reference estimator (VRE) combined with Fuzzy logic control (FLC). (Napole, Derbeli & Barambones, 2021). The implementation of MPPT full bridge converter on MATLAB/Simulink software using two models on DC Nano Grid System also showed an improved efficiency for Fuzzy Type-2 thus: Model 1 – Fuzzy Type-2 (91.40%); Fuzzy Type-1 (80.64%). Model 2 – Fuzzy Type-2 (87.63%);

SCVJ
Volume 4, Issue 2, 2023
DOI: https://doi.org/10.55989/TKOW2858
Science View Journal
ISSN (Online): 2734-2638

Fuzzy Type-1 (77.93%). However, such a system implementation can be undesirably complex. (Prastyawan, Efendi & Murdianto, 2021).

The design and implementation of a linear quadratic regulator (LQR) based maximum power point tracker for solar photovoltaic system, which involved real time experiment and simulation was also carried out by researchers. The results comparison showed a better efficiency than others. That is, P&O: 77.60 – 79.39% Fuzzy Logic: 85.63 – 88.88% LQR: 90.87 – 94.78%. (Karanjkar, Chatterji, Kumar, & 2014). The work of another researcher which involved implementation of LQR-based maximum power point tracking method for standalone photovoltaic system with an experimental validation also showed an improved performance when compared with that of the conventional (P&O) method. The tracking speeds were recorded as LQR (0.04s); P&O (0.165s) while the tracking efficiency were: LQR (96.93%); P&O (91.83%). (Anbarasi, & Kanthalakshmi, 2016). However, the LQR method lacks the tuning mechanism which would enable it to adapt to the changing conditions of the environment.

This paper is therefore aimed at analyzing solar photovoltaic (PV) energy system using model reference adaptive control technique to show the performance of the system. The features or parameters under study in this paper would include efficiency, rise time, duty cycle and the tuning mechanism.

II. Materials and Methods

MATERIALS

The following tools and equipment were used during the course of this work:

i) MATLAB/Simulink software application

ii) Solar photovoltaic (PV) data sheet

iii) MRAC mathematical tools

iv) Internet

METHODS

Data Validation

By using the standard solar photovoltaic model equations(Mboumboue, & Njomo, 2013; Tsai, Tu & Su, 2008; Kachhiya, Lokhande & Patel, 2011),as shown in equations (1), (2), (3) and (4), the characteristic curve was plotted as shown in figuresI and II, by using MATLAB/Simulink environment. To achieve this purpose, the data was obtained from the model $PV - MLU255HC$, with the power rating of $255W$ extracted online from Mitsubishi electric photovoltaic module specification sheet. MATLAB/Simulink was used to simulate the module. The results obtained from the graphs were observed to have validated the data displayed on the specification sheet (https://www.studylib.net/doc/18057350/mlu-specification-sheet-250-255w).

The photocurrent,

$$I_L = I_{sc} + K_i(T_a - T_r) \cdot \frac{\lambda}{1000} \quad (1)$$

The saturation current,

$$I_o = I_{rs}\left(\frac{T_a}{T_r}\right)^3 e^{\left[\frac{qE_{g0}}{nk}\left(\frac{1}{T_r}-\frac{1}{T_a}\right)\right]} \quad (2)$$

The reverse saturation current,

$$I_{rs} = \frac{I_{sc}}{e^{\left(\frac{qV_{oc}}{N_s k n T_a}\right)} - 1} I_{rs} \quad (3)$$

The PV current,

$$I_{PV} = N_p I_{ph} - N_p I_o \left\{ e^{\left[\frac{q(V_{PV}+I_{PV}R_s)}{N_s k n T_a}\right]} - 1 \right\} - \frac{V_{PV} + I_{PV}R_s}{R_p} \quad (4)$$

.

Where: T_r = Module temperature(Kelvin),T_a = Ambient temperature (Kelvin,
I_{sc} = Short circuit curren ,λ = Solar irradiance (W/m^2),
V_{oc} = Open circuit voltage,
qCharge of an electron (1.622×10^{-19}Coulumbs),n = Diode ideality factor ($1 < n < 2$),
E_{g0} = Bandgap energy of semiconductor (1.1eV),
k = Boltzmann's constant ($1.3807\ 10^{-23}$Joules/Kelvin),
K_i = Cell's short − circuit temperature coefficient,
N_s = Number of series cells (36),
N_p = Number of shunt cells (1), V_{PV} = Module voltage,
$I_{ph} = I_L$ = Light generated current, I_o = Saturation current.

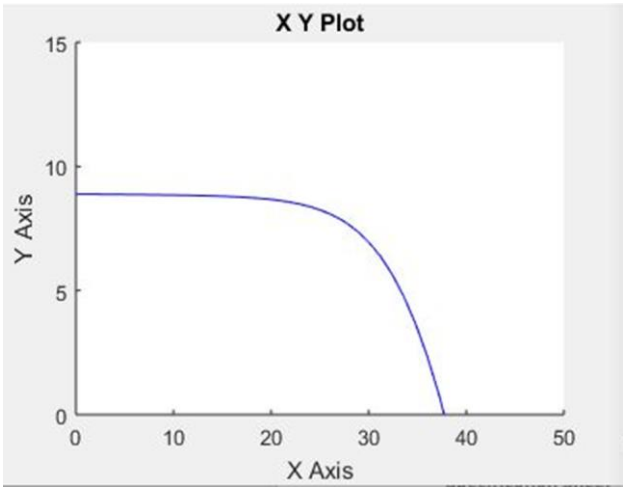

Figure 1: Solar PV Curve Illustrating the I-V Characteristics at Standard Temperature Condition (STC)

SCVJ
Volume 4, Issue 2, 2023
DOI: https://doi.org/10.55989/TKOW2858
Science View Journal
ISSN (Online): 2734-2638

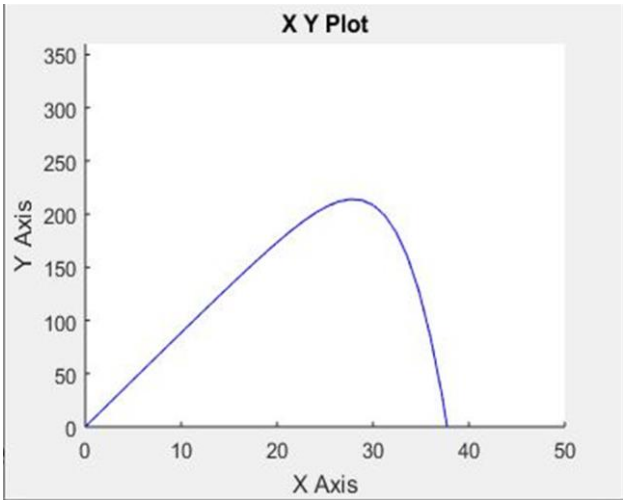

Figure 2: Solar PV Curve Illustrating the P-V Characteristics at Standard Temperature Condition (STC)

Plant Design

The general configuration of a boost converter is illustrated in Figure III. The following assumptions were taken into consideration in the course of the design:

(i) The components are ideal and lossless.
(ii) The time period is T of which switch is closed and opened for periods DT and $(1-D)$, respectively, and operates in Continuous Conduction Mode.
(iii) The capacitor is selected such that the output voltage is constant.

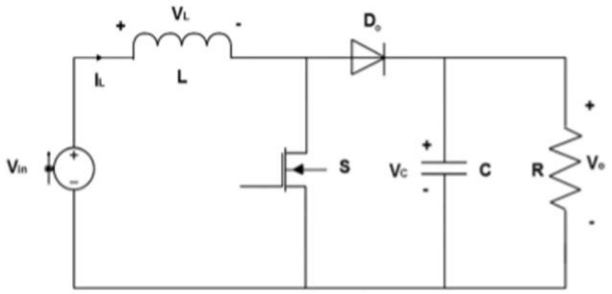

Figure 3: General Configuration of a Boost Converter.

To model the converter, two switch modes were utilized – the on-state and the off-state. The small signal modelling of the converter therefore gives,

$$L\frac{d\hat{\imath}_L}{dt} = \hat{v}_{in} - (1-d)\hat{v}_o + V_o\hat{d} \tag{5a}$$

$$C\frac{d\hat{v}_o}{dt} = (1-d)\hat{\imath}_L - \frac{\hat{v}_o}{R_L} - \hat{\imath}_L\hat{d} \tag{5b}$$

The state space dynamic equation for the system and the output equation obtained from equation (5a) and (5b) by inputting $\hat{\imath}_L = x_1$, $\hat{v}_o = x_2$, are given by

$$\begin{bmatrix}\dot{x}_1\\ \dot{x}_2\end{bmatrix} = \begin{bmatrix}0 & -\frac{1}{L}(1-d)\\ \frac{1}{C}(1-d) & -\frac{1}{CR_L}\end{bmatrix}\begin{bmatrix}x_1\\ x_2\end{bmatrix} + \begin{bmatrix}\frac{V_o}{L} & \frac{1}{L}\\ -\frac{I_L}{C} & 0\end{bmatrix}\begin{bmatrix}\hat{d}\\ \hat{v}_{in}\end{bmatrix} \tag{6a}$$

$$y = x_2 = [0 \quad 1]\begin{bmatrix}x_1\\ x_2\end{bmatrix} \tag{6b}$$

Substituting the values of the parameters shown in Table I, the equation becomes,

$$\begin{bmatrix}\dot{x}_1\\ \dot{x}_2\end{bmatrix} = \begin{bmatrix}0 & -4\times10^3\\ 80 & -8\end{bmatrix}\begin{bmatrix}x_1\\ x_2\end{bmatrix} + \begin{bmatrix}8\times10^5 & 10\times10^3\\ -1.56\times10^3 & 0\end{bmatrix}\begin{bmatrix}\hat{d}\\ \hat{v}_{in}\end{bmatrix} \tag{7a}$$

$$y = x_2 = [0 \quad 1]\begin{bmatrix}x_1\\ x_2\end{bmatrix} \tag{7b}$$

Where the constants, $\bar{A} = \begin{bmatrix}0 & -4\times10^3\\ 80 & -8\end{bmatrix}$, $\bar{B} = \begin{bmatrix}10\times10^3\\ 0\end{bmatrix}$, $\bar{C} = [0 \quad 1]$ and $\bar{D} = 0$

TABLE 1: SUMMARY OF THE BOOST CONVERTER DESIGN SPECIFICATION

Description of component	Rating
Input voltage (V_{in})	$31.2V$
Output capacitance (C)	$5.0mF$
Load resistance (R_L)	25.0Ω
Inductance (L)	$0.1mH$
Nominal duty ratio (D)	0.6
Switching frequency	$20kHz$

MRAC Design

The control section of the system, MRAC was designed by considering the following four steps:

***Step I*:** Expression of the control plant and reference model

Given the process dynamics,

$$Y_p(s) = \frac{k_p}{s^2 + a_p s + b_p}U(s) \tag{8a}$$

and the reference model,

$$Y_m(s) = \frac{k_m}{s^2 + a_m s + b_m}R(s) \tag{8b}$$

In time domain, the equations were respectively presented thus:

$$\ddot{y}_p = -a_p\dot{y}_p - a_p y_p + b_p u \tag{9a}$$

SCVJ
Volume 4, Issue 2, 2023
DOI: https://doi.org/10.55989/TKOW2858
Science View Journal
ISSN (Online): 2734-2638

$$\ddot{y}_m = -a_m\dot{y}_m - a_m y_m + b_p r \quad (9b)$$

Transforming the equations to the first order yields,

$$\dot{y}_p = -A_p y_p + B_p u \quad (10a)$$

$$\dot{y}_m = -A_m y_m + B_m r \quad (10b)$$

$Where:\ A_p = \begin{bmatrix} 0 & -1 \\ b_p & a_p \end{bmatrix};\ A_m = \begin{bmatrix} 0 & -1 \\ b_m & a_m \end{bmatrix};\ B_p = \begin{bmatrix} 0 \\ k_p \end{bmatrix}$ and $B_m = \begin{bmatrix} 0 \\ k_m \end{bmatrix}$

Step II: Determination of control law and adaptation parameters

The control law,

$$u = r\theta_1 - y_p\theta_2 \quad (11)$$

Substituting for u in equation (10a) we get,

$$\dot{y}_p = -(A_p + B_p\theta_2)y_p + B_p\theta_1 r \quad (12)$$

Hence, from equations (9b) and (11), the adaptation parameters,

$$\theta_1 = \frac{B_m}{B_p} \text{and} \theta_2 = \frac{A_m - A_p}{B_p} \quad (13)$$

Step III: Error Analysis

Error equation is given by

$$\boldsymbol{e = y_p - y_m} \quad (14a)$$

$$\boldsymbol{\dot{e} = \dot{y}_p - \dot{y}_m} \quad (14b)$$

Substituting for $\dot{y}_p$ and $\dot{y}_m$, and simplifying we have

$$\dot{e} = -A_m(y_m - y_p) - (B_p\theta_2 + A_p - A_m)y_p + (B_p\theta_1 - B_m)r \quad (15)$$

Step IV: Derivation of the update (adaptation) law

By Lyapunov function,

$$V(e,\theta_1,\theta_2) = \frac{1}{2}\Gamma e^2 + \frac{1}{2B_p}(B_p\theta_1 - B_m)^2 + \frac{1}{2B_p}(B_p\theta_2 + A_p - A_m)^2 \quad (16)$$

Differentiating and further simplification yields,

$$\dot{V}(e,\theta_1,\theta_2) = -\Gamma A_m e^2 + (\Gamma e r + \dot{\theta}_1)(B_p\theta_1 - B_m) + (-\Gamma e y_p + \dot{\theta}_2)(B_p\theta_2 + A_p - A_m) \quad (17)$$

Hence, the update law,

$$\dot{\theta}_1 = -\Gamma e r \quad (18a)$$

$$\dot{\theta}_2 = \Gamma e y_p \quad (18b)$$

Design of Reference Model

The corresponding transfer function for equation (6b) was obtained by using the MATLAB code, $[num, den] = ss2(A, B, C, D)$, which gives,

$$G(s) = \frac{(8 \times 10^5)}{s^2 + 8s + (3.2 \times 10^5)} \quad (19)$$

Comparing the characteristic equation (the denominator) with the canonical form,

$$s^2 + 2\xi\omega_n s + {\omega_n}^2 = 0 \quad (20)$$

Where $\boldsymbol{\xi}$ is the damping ratio and ω_n is the natural frequency

$$\omega_n = 565.69 rad/s \ and \ \ \xi = 0.007 \quad (21)$$

The damping ratio of 0.007 showed an under-damped system. hence, a reference model system was designed by assuming a critically damped system such that ξ = 1, hence the natural frequency was obtained as,

$$\omega_n = 4 \quad (22)$$

The choice of the k_m value (numerator) was made by varying the numerator of the transfer function upon simulation on Simulink. The value of k_m which yielded the response with minimal oscillations was 20. This value must be chosen such that $k_m \geq {\omega_n}^2$ = 16. From the result, the reference model system was determined as,

$$G(s) = \frac{20}{s^2 + 8s + 16} \quad (23)$$

Figure IV shows the Simulink model created from the mathematical models obtained above.

SCVJ
Volume 4, Issue 2, 2023
DOI: https://doi.org/10.55989/TKOW2858
Science View Journal
ISSN (Online): 2734-2638

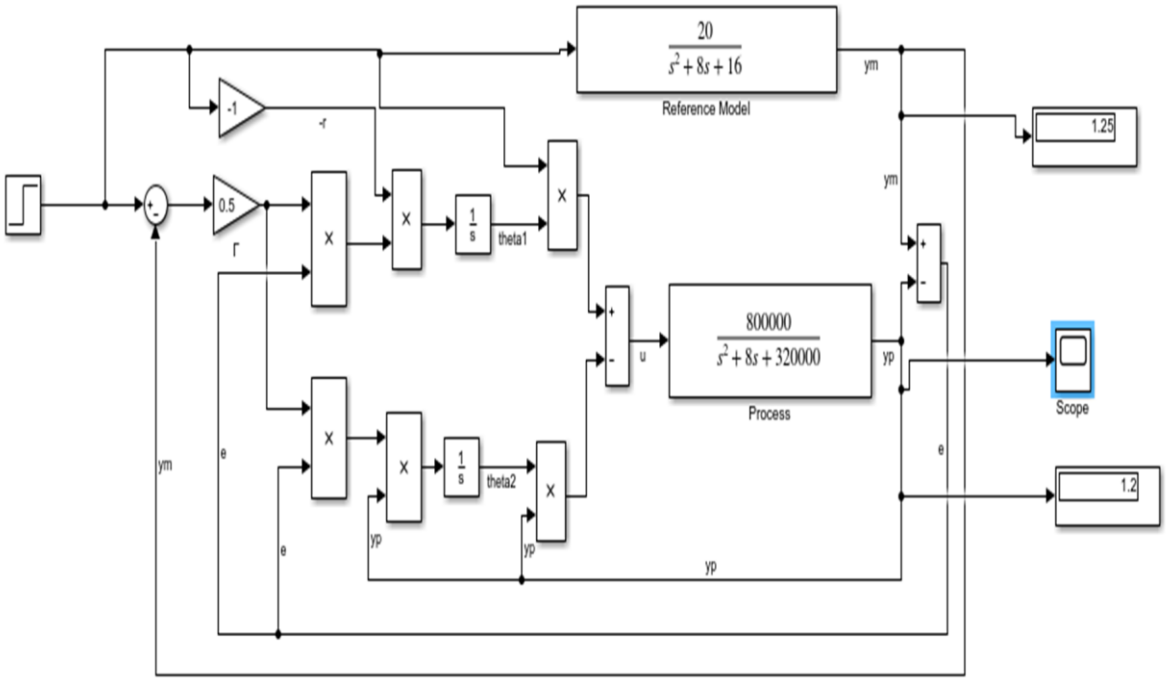

Figure 4: Simulink Model of MRAC-Only Control Scheme.

III. Results

The system was simulated using the Simulink model shown in Figure IV and the results were plotted as shown in Figures V, VI, VII, VIII and IX, which depict the time response for different gain values. Table II shows the summary of the performance for the system as per different gain values while Table III shows the summary of the performance result measured from the plotted graph. Such parameters considered were efficiency, duty cycle, rise time and adaptation gain values.

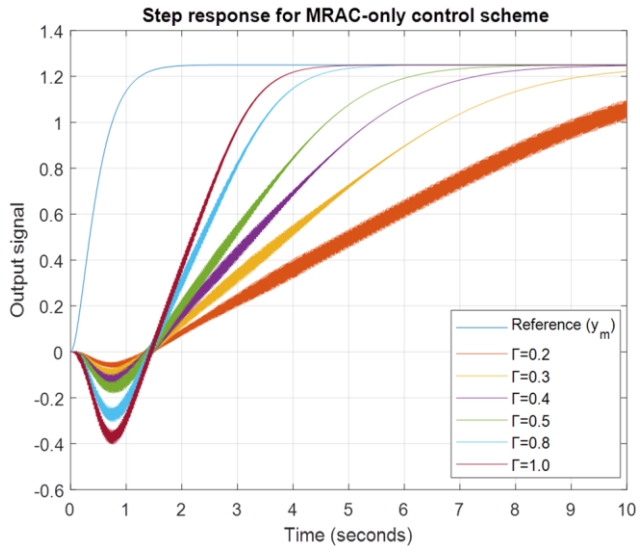

Figure 5: Time Response Curve Illustrating the Output Signal for Different Gain Values.

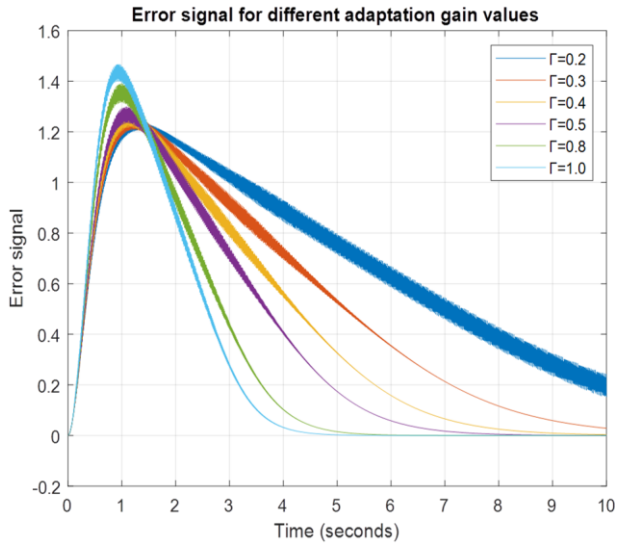

Figure 6: Time Response Curve Illustrating the Output Error for Different Gain Values.

SCVJ
Volume 4, Issue 2, 2023
DOI: https://doi.org/10.55989/TKOW2858
Science View Journal
ISSN (Online): 2734-2638

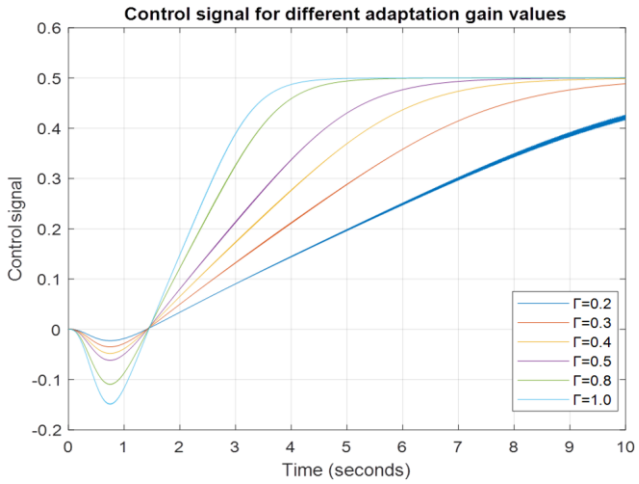

Figure 7: Time Response Curve Illustrating the Control Signal for Different Gain Values.

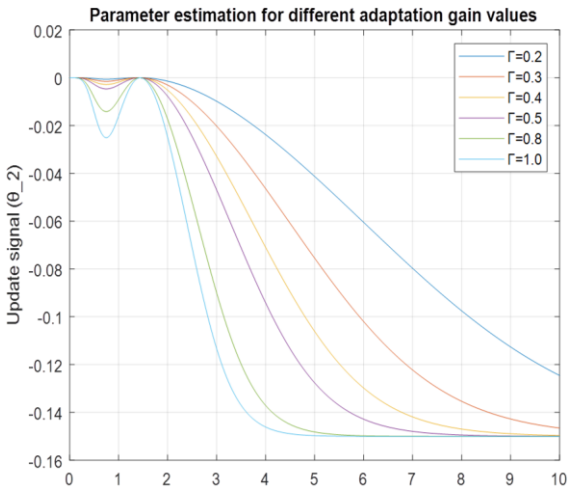

Figure 8: Parameter Estimation Illustrating Update Law $[\theta_2]$ for Different Gain Values.

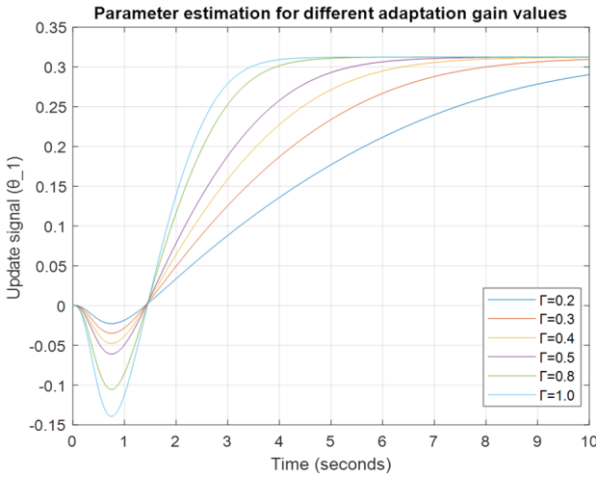

Figure 8: Parameter Estimation Illustrating Update Law $[\theta_1]$ for Different Gain Values.

TABLE 2: SYSTEM PERFORMANCE AS PER DIFFERENT ADAPTATION GAINS

Adaptation Gain	θ_1	θ_2	Rise time (s)	Overshoot (%)	Steady state
0.005	0.032	-0.0002139	3.083	-96.5	0.008861
0.05	0.117	-0.01745	2.662	-78.0	0.2806
0.1	0.2028	-0.05511	4.704	-71.6	0.6232
0.2	0.2903	-0.1245	5.964	4.9	1.093
0.3	0.3097	-0.1463	5.475	21.5	1.227
0.4	0.3121	-0.1497	4.506	24.0	1.247
0.5	0.3124	-0.15	3.666	20.4	1.25
0.6	0.3124	-0.1501	2.855	23.9	1.25
0.7	0.3124	-0.1501	2.74	25.0	1.25
0.8	0.3124	-0.15	2.133	25.0	1.25
0.9	0.3124	-0.1501	1.899	25.2	1.25
1.0	0.3124	-0.1501	2.049	24.2	1.25
1.5	0.3124	-0.1501	1.173	24.6	1.254
1.8	0.3123	-0.1501	1.476	24.0	1.243
1.9	0.3134	-0.1492	1.323	20.7	1.192

SCVJ
Volume 4, Issue 2, 2023
DOI: https://doi.org/10.55989/TKOW2858

Science View Journal
ISSN (Online): 2734-2638

TABLE 3: SUMMARY OF THE MEASURED PARAMETERS

Parameter	Values
Efficiency (η)	73.41%
Duty cycle (d)	0.714
Rise time	2.938s
Adaptation gain	$0.2 < \Gamma < 2$

IV. Discussion

Figure V illustrates the time response of the model reference adaptive control (MRAC) scheme used in controlling the solar PV system. The system was observed to have converged at an output signal value of 1.2, which is the steady state value of the system, while the control signal showed a value of 0.5 as depicted in Figure VII. According to the graphs, as the adaptation gain increases the rise time decreases, which implies the decrease in the convergence speed. Figure VI also illustrates the error between the reference signal and the output signal at different gain values. The error signals were observed to have converged to zero but at different times depending on the gain value. Figures VIII and IX illustrates how the system adapts to the changing conditions of the environment as the adaptation gains vary. As one update law was increasing the other one was decreasing in order to minimize the error signal to zero. Table II summarizes how the update laws vary to compensate for the changing condition of the environment.

The unique feature of MRAC system is its ability to adjust itself at a changing condition of the environment. The simulation results show that the system was able to adapt to the changing condition as expected but the adaptation gain must be kept small within the limit ($0.2<\Gamma<2$) to avoid oscillations of the system just as pointed out in a research work by (Jain & Niga, 2013). This implies that the system would operate as expected within the range of the adaptation gain hence, beyond this range the system would not operate accurately. It was also observed that with this control method, the system was able to track the maximum power point (MPP) at average rise time of 2.938s as suggested by Khanna, et al. (2014). The rise time is the time required for a system to rise from 10% to 90% of its steady state value. Therefore, the rise time obtained implies that the system is able to converge at its final value within 2.938s. MRAC scheme gives a tracking efficiency of 73.41%, and a duty cycle of approximately of 0.7. The implication of the duty cycle is that the system is capable of working for about 70% of the entire period while the remaining 30% is for the discharging. For future directions, it is suggested that it is necessary to improve on the adaptation gain values so that the system can remain accurately operatable even at large adaptation gains.

V. Conclusion

This paper presents the maximum power point tracking improvement using model reference adaptive control (MRAC) technique. To achieve this, data were required for the design hence, the use of the model, $PV - MLU255HC$ taken from MITSUBISHI electric module specification. To ensure that the data extracted from the data sheet were correct, validation was carried out by modelling a Simulink block from standard solar photovoltaic model equations. The system was developed by considering the design of the plant, the design of the control system and simulation of the results. The result analysis shows that the MRAC system is capable of adapting to environmental uncertainties at small adaptation gains not exceeding the range ($0.2<\Gamma<2$). Moreover, other performance parameters determined were efficiency of 73.41%, a rise time of 2.938s, which depicts the tracking speed, and a duty cycle of 0.7, which implies the working time of the controller. However, though the system is capable of adjusting itself at changing conditions, it would be a great idea if the system is worked upon to improve the adaptation gains in the future research.

VI. Acknowledgements

We express our profound gratitude to the Almighty God for His Grace towards the success of this work. We wish to appreciate our friends, colleagues, and so on including Mfonobong Eleazar Benson, for their contributions in ideas and knowledge, during the course of this work at Federal University of Technology, Owerri, Nigeria.

VII. References

Anbarasi, M. and Kanthalakshmi, S. (2016). "Linear quadratic optimal control of solar photovoltaic system: An experimental validation." Journal of Renewable and Sustainable Energy. Vol. 8. http://dx.doi.org/10.1063/1.4966229.

Dolara, A., Faranda, R. and Leva, S. (2009). "Energy comparison of seven MPPT techniques for PV systems." Journal of Electromagnetic Analysis and Applications. Vol. 1, No. 3, pp.152– 162.

Jain, P. and Nigam, M. J. (2013). "Design of a Model Reference Adaptive Controller Using Modified MIT Rule for a Second Order System." Advance in Electronic and Electric Engineering. ISSN 2231-1297, Vol. 3, No. 4, pp. 477-484 © Research India Publications http://www.ripublication.com/aeee.htm.

Kachhiya, K., Lokhande, M. and Patel, M., (2011). "MATLAB/Simulink Model of Solar PV Module and MPPT Algorithm." National Conference on Recent Trends in Engineering & Technology. B. V. M. Engineering College, V. V. Nagar, Gujarat India, pp. 1-5, 13-14.

Karanjkar, D. S., Chatterji, S. and Kumar, A. (2014). "Design and Implementation of a Linear Quadratic Regulator Based Maximum Power Point Tracker for Solar Photo-Voltaic System." International Journal of Hybrid Information Technology. Vol.7, No.1, pp. 167- 182. http://dx.doi.org/10.14257/ijhit.2014.7.1.14. ISSN: 1738-9968 IJHIT Copyright ⓒ 2014 SERSC.

Khanna, R., Zhang, Q., Stanchina, W. E., Reed, G. F. and Mao, Z. (2014). "Maximum Power Point Tracking Using Model Reference Adaptive Control." IEEE Transactions on Power Electronics. Vol. 29, No. 3, pp. 1490 – 1499.

DOI: https://doi.org/10.55989/TKOW2858

Mboumboue, E. and Njomo, D. (2013). "Mathematical Modeling and Digital Simulation of PV Solar Panel using MATLAB Software." International Journal of Emerging Technology and Advanced Engineering. Vol. 3, Issue 9, pp. 24 – 32. Website: www.ijetae.com (ISSN 2250- 2459, ISO 9001:2008 Certified Journal).

Mitsubishi Photovoltaic Module specification sheet (MLU): 250-255W[online], https://www.studylib.net/doc/18057350/mlu-specification-sheet-250-255w.

Napole, C., Derbeli, M. and Barambones, O. (2021). Fuzzy Logic Approach for Maximum Power Point Tracking Implemented in a Real Time Photovoltaic System. Journal of Applied Sciences. Vol. 11, No. 5927 pp. 1 – 18. https://doi.org/10.3390/app11135927;https://www.mdpi.com/journal/applsci.

Prastyawan, A., Efendi, M. and Murdianto, F. (2021). "MPPT Full Bridge Converter Using Fuzzy Type-2 on DC Nano Grid System." Journal on Advanced Research in Electrical Engineering. Vol. 5, No. 2, pp. 120 – 127.

Tsai, H., Tu, C. and Su, Y. (2008). "Development of Generalized Photovoltaic Model Using MATLAB/SIMULINK." Proceedings of the World Congress on Engineering and Computer Science, WCECS 2008, San Francisco USA, pp. 1-6.

Vyshnavi, N. and Subramanian, K. (2015). "Model reference adaptive control for maximum power point tracking in PV systems." IJARIIE - ISSN(O) – 2395-4396. Vol-1 Issue-5, pp. 556 – 568. www.ijariie.com.